Mixed alkali effect in borate glasses - electron paramagnetic resonance and optical absorption studies in Cu2+ doped xNa2O– (30 − x)K2O– 70B2O3 glasses

2003 J. Phys.: Condens. Matter 15 1469

(http://iopscience.iop.org/0953-8984/15/9/311)

INSTITUTE OF PHYSICS PUBLISHING JOURNAL OF PHYSICS: CONDENSED MATTER

J. Phys.: Condens. Matter **15** (2003) 1469–1486 PII: S0953-8984(03)39665-1

Mixed alkali effect in borate glasses—electron paramagnetic resonance and optical absorption studies in Cu^{2+} doped $x$$Na_2O$–(30 − x)K_2O–70B_2O_3 glasses

R P Sreekanth Chakradhar[1], **K P Ramesh**[1], **J L Rao**[2] **and J Ramakrishna**[1]

[1] Department of Physics, Indian Institute of Science, Bangalore-560012, India
[2] Department of Physics, S V University, Tirupati-517502, India

E-mail: chakra72@physics.iisc.ernet.in and jr@physics.iisc.ernet.in (J Ramakrishna)

Received 18 July 2002, in final form 8 January 2003
Published 24 February 2003
Online at stacks.iop.org/JPhysCM/15/1469

Abstract

The mixed alkali borate glasses $x$$Na_2O$–(30 − x)K_2O–70B_2O_3 ($5 \leqslant x \leqslant 25$), doped with 0.5 mol% of CuO, have been investigated, using electron paramagnetic resonance (EPR) and optical absorption techniques, as a function of mixed alkali content, to look for the 'mixed alkali effect' (MAE) on the spectral properties of the glasses. The EPR spectra of all the investigated samples exhibit resonance signals which are characteristic of the Cu^{2+} ions in octahedral sites with tetragonal distortion. From the observed EPR spectra, the spin-Hamiltonian parameters have been determined. It is observed that the spin-Hamiltonian parameter $g_{\parallel}$ goes through a minimum around $x = 10$–15 whereas $A_{\parallel}$ goes through a maximum around $x = 15$ showing the MAE. The number of spins participating in resonance (N_2) and the calculated paramagnetic susceptibilities (χ) exhibit a shallow minimum around $x = 20$ showing the MAE in these glasses. The optical absorption spectrum of the $x = 5$ glass exhibits two bands: a strong band centred at 14 240 cm^{-1} corresponding to the transition ($^2B_{1g} \rightarrow {}^2B_{2g}$) and a weak band on the higher energy side at 22 115 cm^{-1} corresponding to the transition ($^2B_{1g} \rightarrow {}^2E_g$). With $x > 5$, the higher energy band disappears and the lower energy band shifts slightly to the lower energy side. By correlating the EPR and optical absorption data, the molecular orbital coefficients α^2 and β_1^2 are evaluated for the different glasses investigated. The values indicate that the in-plane σ bonding is moderately covalent while the in-plane π bonding is significantly ionic in nature; these exhibit a minimum with $x = 15$, showing the MAE. The theoretical values of optical basicity of the glasses have also been evaluated. From optical absorption edges, the optical bandgap energies have been calculated and are found to lie in the range 3.00–3.40 eV. The physical properties of the glasses studied have also been evaluated with respect to the composition.

Table 1. Composition of glasses (mol%) studied in the present work.

Glass code, x	Glass system
5	$5Na_2O$–$25K_2O$–$69.5B_2O_3$–0.5CuO
10	$10Na_2O$–$20K_2O$–$69.5B_2O_3$–0.5CuO
15	$15Na_2O$–$15K_2O$–$69.5B_2O_3$–0.5CuO
20	$20Na_2O$–$10K_2O$–$69.5B_2O_3$–0.5CuO
25	$25Na_2O$–$5K_2O$–$69.5B_2O_3$–0.5CuO

1. Introduction

The mixed alkali effect is one of the classic 'anomalies' of glass science [1–5] and has been the subject of study over the years. Many physical properties of oxide glasses show non-linear behaviour exhibiting a minimum or maximum, as a function of alkali content, if one alkali ion is gradually replaced by another alkali ion, keeping the total alkali content constant. This behaviour is called the 'mixed alkali effect' (MAE), and is observed for properties associated with alkali ion movement such as electrical conductivity, ionic diffusion, dielectric relaxation and internal friction [1]. The MAE is not much studied using spectroscopic techniques, but they would be important and useful to gain insight into the microscopic mechanisms responsible for the effect.

The studies of transition metal ions in glasses by EPR and optical absorption techniques give information on the structure of the glass. The changes in the composition of the glass may change the local environment of the transition metal ion incorporated into the glass, leading to ligand field changes which may be reflected in the EPR and optical absorption spectra. As mentioned above, spectral investigations of the MAE are very meagre. Only optical absorption of Cu and Ni doped in a few mixed alkali silicate glasses and that of Cu doped in a couple of mixed alkali borate glasses have been reported [6–9]. Thus, a systematic study of the spectral characteristics in mixed alkali glasses is necessary to evolve a consistent understanding of the MAE in glasses. Borate glasses are interesting systems as they undergo many structural changes with composition and systematic investigation of the MAE in them should be interesting. As a part of such a programme, we have investigated sodium potassium borate glasses (hereafter referred to as NaKB) doped with Cu^{2+} ions using EPR and optical absorption techniques and the results obtained from these studies are discussed with respect to the composition of the mixed alkali elements.

2. Experimental techniques

The starting materials M_2CO_3 (M = Na or K), H_3BO_3 and CuO, used in the preparation of the glasses, were of analar grade quality. Table 1 lists the batch composition in mol% of glasses studied in the present work. The chemicals were weighed accurately in an electronic balance, mixed thoroughly and ground to fine powder. The batches were then placed in porcelain crucibles and melted in an electrical furnace in air at 1000 °C for half an hour. The melt was then quenched to room temperature in air by pouring it onto a polished porcelain plate and pressing it with another porcelain plate. The glasses thus obtained were blue in colour with good optical quality and high transparency. The glasses were then annealed at 150 °C. The glass formation was confirmed by powder x-ray diffraction recorded with a Phillips type PW 1050 diffractometer using Cu Kα radiation.

The EPR spectra were recorded on an EPR spectrometer (JEOL-FE-1X) operating in the X-band frequency ($\approx$9.200 GHz) with a field modulation frequency of 100 kHz. The magnetic

field was scanned from 0 to 500 mT and the microwave power used was 5 mW. A powdered glass sample of 100 mg was placed in a quartz tube for EPR measurements. The optical absorption spectra of the glasses were recorded using a JASCO UV–VIS–NIR spectro-photometer in the wavelength region 300–900 nm.

2.1. Physical properties of copper doped mixed alkali borate glasses

By using the Archimedes principle, the glass densities have been determined with xylene as the immersion liquid on a single-pan electrical balance to the nearest 0.000 01 g. The error in density measurement is estimated to be ± 0.004 g cm^{-3}. The corresponding molar volumes have also been calculated. It is observed that the density increases with x and reaches a maximum for $x = 15$, and thereafter it decreases, showing the MAE.

The glass refractive indices have been measured using an Abbe refractometer with a sodium vapour lamp ($\lambda = 589.3$ nm) with an accuracy of ± 0.001. The sample being glassy, it requires an adhesive coating on its surface, preferably 1-monobromonaphthalene, as its refractive index is close to that of a conventional glass.

The dielectric constant (ε) was calculated from the refractive index of the glass using [10].

$$\varepsilon = n_d^2. \tag{1}$$

The reflection loss from the glass surface was computed from the refractive index by using the Fresnel formula as shown below [11]:

$$R = \left[\frac{(n_d - 1)}{(n_d + 1)}\right]^2. \tag{2}$$

The molar refractivity R_M for each glass was evaluated using [12]

$$R_m = \left[\frac{(n_d - 1)}{(n_d + 2)}\right]\frac{M}{D} \tag{3}$$

where M is the average molecular weight and D is the density in g cm^{-3}.

The electronic polarizability α_e was calculated using the formula [13]

$$\alpha_e = \frac{3(n_d^2 - 1)}{4\pi N(n_d^2 + 2)} \tag{4}$$

where N is the number of copper ions per unit volume.

The polaron radius and inter-ionic separation were calculated using the formulae [14]

$$r_p = \frac{1}{2}\left(\frac{\pi}{6N}\right)^{1/3} \tag{5}$$

and

$$r_i = \left(\frac{1}{N}\right)^{1/3} \tag{6}$$

where $\pi = 3.141$ is a constant. From table 2 it is observed that the densities, concentration and field strength increase with x and reach a maximum at $x = 15$ and thereafter decrease, showing the MAE. However the molar refractivity (R_m), mean atomic volume (V), electronic polarizability (α_e), ionic radius (r_P) and inter-ionic distance (r_i) slightly decrease and exhibit a minimum at $x = 15$, showing the MAE in these glasses.

Table 2. Certain physical parameters of Cu^{2+} ion doped mixed alkali borate glasses.

Serial no	Physical property	Glass code, x				
		5	10	15	20	25
1	Average molecular weight	83.22	81.615	79.998	78.388	76.776
2	Density, D (g cm^{-3})	2.358	2.483	2.774	2.530	2.409
3	Refractive index, n_D	1.514	1.512	1.510	1.508	1.503
4	Molar refractivity, R_m (cm^{-3}) (±0.005)	10.625	9.863	8.625	9.230	9.421
5	Mean atomic volume, V (g cm^{-3}/atom) (±0.025)	0.0805	0.0749	0.0657	0.0706	0.0726
6	Optical dielectric constant, $(\varepsilon - 1)(\pm 0.05)$	1.292	1.286	1.280	1.274	1.259
7	Electronic polarizability, α_e (10^{-24} ions cm^{-3}) (±0.005)	8.420	7.816	6.825	6.919	7.466
8	Concentration, N (10^{21} ions cm^{-3}) (±0.005)	8.535	9.165	10.445	10.285	9.452
9	Optical basicity (Λ_{th})	0.4014	0.3969	0.3924	0.3880	0.3837
9	Ionic radius, r_P (Å) (±0.02)	1.97	1.92	1.84	1.85	1.91
10	Inter-ionic distance, r_i (Å) (±0.05)	4.89	4.77	4.57	4.59	4.73
11	Field strength F (10^{15} cm^2) (±0.005)	5.153	5.425	5.907	5.843	5.482

2.2. Optical basicity of the glass (Λ_{th})

The optical basicity of an oxide glass will reflect the ability of the glass to donate negative charge to the probe ion [15]. Duffy and Ingram [16] reported that the ideal values of optical basicity can be predicted from the composition of the glass and the basicity moderating parameters of the various cations present. The theoretical values of optical basicity of the glass can be estimated using the formula [16]

$$\Lambda_{th} = \sum_{i=1}^{n} \frac{Z_i r_i}{2\gamma_i} \tag{7}$$

where n is the total number of cations present, Z_i is the oxidation number of the ith cation, r_i is the ratio of the number of ith cations to the number of oxides present and γ_i is the basicity moderating parameter of the ith cation. The basicity moderating parameter γ_i can be calculated [16] from the following equation:

$$\gamma_i = 1.36(x_i - 0.26) \tag{8}$$

where x_i is the Pauling electronegativity [17] of the cation. The theoretical values of optical basicity (Λ_{th}) were calculated for all the glass samples and are listed in table 2. It is found that the optical basicity of the glasses decreases with increase of x.

3. Results and discussion

3.1. X-ray diffraction

The x-ray diffraction pattern of an amorphous material is distinctly different from that of crystalline material and consists of a few broad diffuse haloes rather than sharp rings. All the samples were tested and the results showed the absence of crystalline characteristics. Figure 1

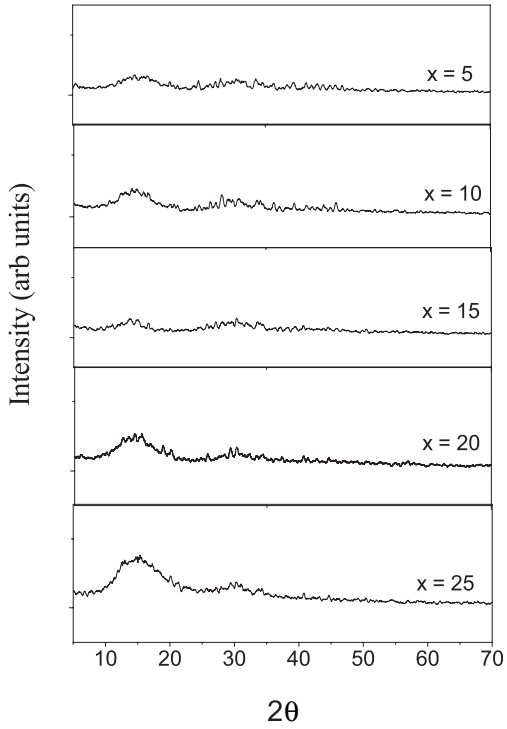

Figure 1. X-ray diffraction pattern for different mixed alkali borate glasses $x$$Na_2O$–$(30 - x)K_2O$–$69.5B_2O_3 + 0.5CuO$ ($5 \leqslant x \leqslant 25$), at room temperature.

shows the typical x-ray diffraction patterns for these compositions (see table 1). The patterns obtained did not reveal any crystalline phase in the glass. The intensity of the broad peak at $2\theta \approx 15$ goes through a minimum for $x = 15$ and it is interesting to note that this may be due to the MAE.

3.2. EPR studies

No EPR signal was detected in the spectra of undoped glasses, indicating that there are no paramagnetic impurities present in the starting materials. When Cu^{2+} ions were added to the NaKB glasses, the EPR spectra exhibit resonance signals similar to those reported for Cu^{2+} ions in other glass systems [18–42].

Figure 2 shows the EPR spectra of 0.5 mol% of copper ions in NaKB glasses with different compositions of mixed alkalis at 300 K. The Cu^{2+} ion with $S = 1/2$ has a nuclear spin $I = 3/2$ for both ^{63}Cu (natural abundance 69%) and ^{65}Cu (natural abundance 31%) and therefore $(2I + 1)$, i.e. four parallel and four perpendicular, hyperfine components would be expected. In the recorded spectra, we observed three weak parallel components in the lower field region and the fourth parallel component is overlapped with the perpendicular component; the perpendicular components in the high field region are well resolved. It can be observed that the high field side of the spectrum is more intense than the low field side.

For Cu^{2+} ions, a regular octahedral site may not exist, as the cubic symmetry is disturbed by the electronic hole in the degenerate $d_{x^2-y^2}$ orbital and this produces the tetragonal distortion. The EPR spectra of Cu^{2+} ions in the glasses studied could be analysed by using an axial spin

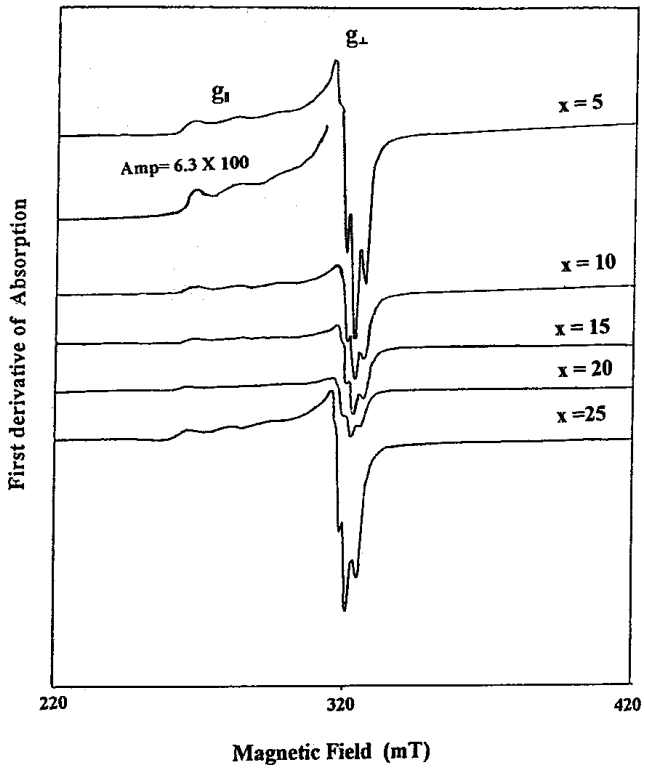

Figure 2. EPR spectra of 0.5 mol% Cu^{2+} ions doped in different mixed alkali borate glasses xNa$_2$O–(30 − x)K$_2$O–70B$_2$O$_3$ ($5 \leqslant x \leqslant 25$), at room temperature.

Hamiltonian [43]. The solution of the spin Hamiltonian gives the expressions for the peak positions related to the principal 'g' and 'A' tensors [44].

The spin-Hamiltonian parameters have been evaluated and are presented in table 3 (the errors in g and A values are ± 0.001 and $\pm 3 \times 10^{-4}$ respectively). These spin-Hamiltonian parameters are compared with other glass systems (table 3) and are in good agreement with those reported in the literature. As $g_\parallel > g_\perp > g_e$ (free electron g value, $g_e = 2.0023$), the ground state of the paramagnetic electron is $d_{x^2-y^2}$ ($^2B_{1g}$ state), the Cu^{2+} ion being located in distorted octahedral sites (D_{4h}) elongated along the z-axis [18, 20]. In the mixed alkali borate (NaKB) glasses we have observed the relation $g_\parallel > g_\perp > g_e$ and the observed $g_\parallel$ and $g_\perp$ values are characteristic of Cu^{2+} ions co-ordinated by six ligands which form an octahedron elongated along the z-axis. From table 3, it is clear that the coordination structure of isolated Cu^{2+} complexes keeps approximately the same symmetry. However, micro-environmental fluctuations around the Cu^{2+} may also exist which in turn reflects on the spin-Hamiltonian parameters as a function of x. Figure 3 shows the variation of $g_\parallel$ and $A_\parallel$ as a function of x. It is quite interesting to note that in the present system $g_\parallel$ seems go through a minimum around $x = 10$–15 whereas $A_\parallel$ seems to go through a maximum around $x = 15$, showing MAE.

Biswas *et al* [34] have reported in NaF–B$_2$O$_3$ glasses that $g_\parallel$ decreases with increase of NaF content while $A_\parallel$ increases. A steep fall is observed in $g_\parallel$ for NaF content of 15–30 mol% and a slow rise in $A_\parallel$. They attributed the steep change in $g_\parallel$ is indicative of boron anomaly. In NaF–Na$_2$O–B$_2$O$_3$ glasses the authors [34] reported a gradual fall in $g_\parallel$ and a continuous rise in the value of $A_\parallel$ with increasing NaF content. In both the systems the authors reported the

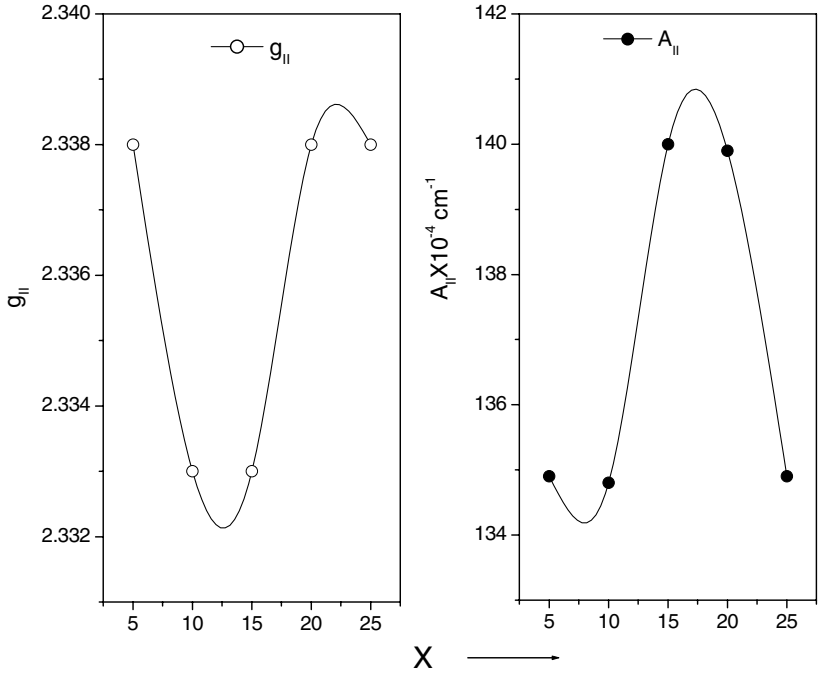

Figure 3. The variation of spin-Hamiltonian parameters $g_\parallel$ and $A_\parallel$ with x in different mixed alkali borate glasses xNa$_2$O–$(30-x)$K$_2$O–69.5B$_2$O$_3$ + 0.5CuO ($5 \leqslant x \leqslant 25$), at room temperature.

values of $g_\parallel$, $A_\parallel$ and $A_\perp$ show a perceptible change indicating a general trend with increasing NaF content, while there is no appreciable change in the values of $g_\perp$. Abrupt or stepwise changes in $g_\parallel$ and $A_\parallel$ have been reported by several research workers [18, 20] in systems showing the borate anomaly. Ramadevudu *et al* [40] also reported $g_\parallel$ and $A_\parallel$ are found to be dependent on the glass composition while $g_\perp$ and $A_\perp$ are essentially constant. They reported that in MgO–Na$_2$O–B$_2$O$_3$ ternary glasses as the MgO content increases $g_\parallel$ decreases and $A_\parallel$ increases which are attributed to the structural changes in the glass.

In the present investigation we have observed the MAE on the spin-Hamiltonian parameters ($g_\parallel$ and $A_\parallel$) as $g_\parallel$ goes through a minimum around $x = 10$–15 whereas $A_\parallel$ goes through a maximum around $x = 15$ (figure 3). These changes are due to structural changes taking place with composition and also modification of the boron network with alkali content. However, $g_\perp$ and $A_\perp$ do not show any clear dependence on x.

3.3. Calculation of number of spins participating in resonance

The number of spins participating in resonance can be calculated by comparing the area under the absorption curve with that of a standard (CuSO$_4$·5H$_2$O in this study) of known concentration. Weil *et al* [45] gave the following expression which includes the experimental parameters of both sample and standard.

$$N_2 = \frac{A_x(\text{scan}_x)^2 G_{std}(B_m)_{std}(g_{std})^2[S(S+1)]_{std}(P_{std})^{1/2}}{A_{std}(\text{scan}_{std})^2 G_x(B_m)_x(g_x)^2[S(S+1)]_x(P_x)^{1/2}}[\text{std}] \tag{9}$$

where A is the area under the absorption curve which can be obtained by double integrating the first derivative EPR absorption curve, 'scan' is the magnetic field corresponding to unit

Table 3. Comparison of spin-Hamiltonian parameters of Cu^{2+} ions in different systems.

System	$g_\parallel$	$g_\perp$	$A_\parallel$ (10^{-4} cm^{-1})	$A_\perp$ (10^{-4} cm^{-1})	References
Li_2O–B_2O_3	2.328	2.050	157	24.9	[28]
Na_2O–B_2O_3	2.327	2.065	150	26.0	[21]
ZnO–B_2O_3	2.321	2.039	159	—	[29]
PbO–B_2O_3	2.323	2.042	152	—	[29]
Li_2O–Na_2O–B_2O_3	2.382	2.061	162	22.5	[30]
$CdSO_4$–B_2O_3	2.422	2.084	77	—	[33]
Li_2SO_4–$CdSO_4$–B_2O_3	2.421	2.089	77	—	[33]
Na_2SO_4–$CdSO_4$–B_2O_3	2.420	2.086	77	—	[33]
K_2SO_4–$CdSO_4$–B_2O_3	2.420	2.089	77	—	[33]
Cs_2SO_4–$CdSO_4$–B_2O_3	2.421	2.086	77	—	[33]
K_2SO_4–$ZnSO_4$	2.438	2.068	90	—	[26]
Na_2SO_4–$ZnSO_4$	2.350	2.070	107	—	[32]
Li_2CO_3–$BaCO_3$–H_3BO_3	2.284	2.053	131	25	[36]
Na_2CO_3–$BaCO_3$–H_3BO_3	2.262	2.049	137	24	[36]
K_2CO_3–$BaCO_3$–H_3BO_3	2.259	2.048	114	24	[36]
$Li_2B_4O_7$–PbO–TeO_2	2.323	2.067	129	22	[37]
$Na_2B_4O_7$–PbO–TeO_2	2.293	2.056	136	23	[37]
$K_2B_4O_7$–PbO–TeO_2	2.291	2.051	130	26	[37]
$Li_2B_4O_7$–TeO_2	2.310	2.063	117	26	[37]
$Na_2B_4O_7$–TeO_2	2.303	2.060	122	24	[37]
$K_2B_4O_7$–TeO_2	2.294	2.056	129	25	[37]
MgO–P_2O_5	2.417	2.059	109	—	[24]
Na_2O–P_2O_5	2.423	2.088	107	—	[42]
CaO–P_2O_5	2.408	2.059	109	—	[24]
SrO–P_2O_5	2.342	2.063	109	—	[24]
BaO–P_2O_5	2.408	2.058	108	—	[24]
ZnO–P_2O_5	2.415	2.058	109	—	[25]
CdO–P_2O_5	2.404	2.058	109	—	[25]
$x Na_2O$–$(30-x)K_2O$–$70B_2O_3$					
$x = 5$	2.338	2.046	134.9	23.7	This work
$x = 10$	2.333	2.043	134.8	23.7	This work
$x = 15$	2.333	2.044	140.0	23.7	This work
$x = 20$	2.338	2.044	139.9	23.7	This work
$x = 25$	2.338	2.045	134.9	23.5	This work

length of the chart, G is the gain, B_m is the modulation field width, g is the g factor and S is the spin of the system in its ground state. P is the power of the microwave source. The subscripts 'x' and 'std' represent the corresponding quantities for the Cu^{2+} glass sample and the reference ($CuSO_4{\cdot}5H_2O$) respectively.

It is interesting to note that the number of spins participating in resonance shows MAE in these glasses and this is shown in figure 4. From the figure it is observed that the number of spins participating in resonance decreases with x (alkali content) and reaches a minimum around $x = 20$ and thereafter increases with x showing the MAE in the glasses. The variation may be due to the structural changes with composition and also the modification of boron network with alkali content.

In B_2O_3 glass, addition of network modifiers (Na_2O and K_2O) leads to an increase in the coordination number of some of the boron atoms from three to four. It is assumed that the

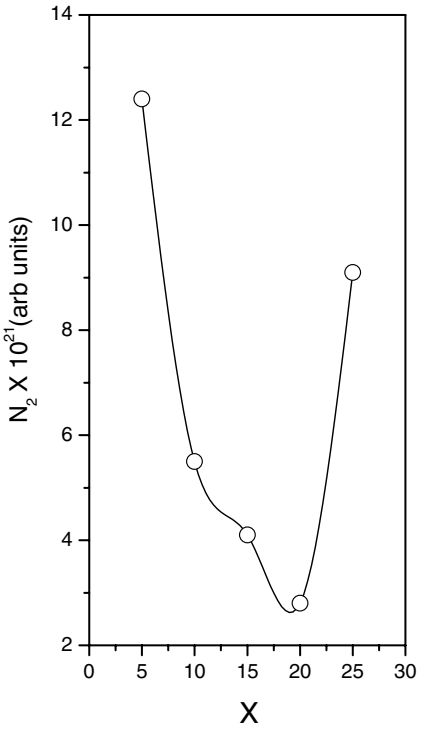

Figure 4. The variation of number of spins (N_2) with x in different mixed alkali borate glasses xNa$_2$O–$(30-x)$K$_2$O–69.5B$_2$O$_3$ + 0.5CuO ($5 \leqslant x \leqslant 25$), at room temperature.

resulting glass is composed of both triangular and tetrahedral units which form a relatively open network with holes between the oxygen atoms of sufficient size to accommodate the Na and K ions. Thus sufficient non-bridging oxygens are available for good coordination in the broken network. The alkali oxides Na_2O and K_2O make available additional weakly bonded O^{2-} for each Cu^{2+}, i.e., Cu^{2+} captures the O^{2-} from Na_2O and K_2O and this happens at the expense of Na_2O and K_2O coordination. Na^+ and K^+ should remain in the neighbourhood of the next stronger Cu^{2+} rather than being incorporated separately into the rigid network. The configurations of Na–O–Cu and K–O–Cu are energetically favoured. Replacement of Na_2O by K_2O causes a smooth change in property–composition curves attaining a value to a maximum or minimum depending on the property.

The number of copper ions was calculated from the density measurements and will be the sum of the copper ions in +2 oxidation state (N_2) and the copper ions in the +1 oxidation state (N_1). Since the EPR technique is only sensitive to copper ions in +2 oxidation state, the number of spins (N_2) is also indicated in table 4. From these two numbers the ratio of the number of copper ions in the +2 state to the total number of copper ions ($N_T = N_1 + N_2$) is calculated (i.e., N_2/N_T) and is also presented in table 4.

3.4. Calculation of paramagnetic susceptibility from EPR data

The EPR data can be used to calculate the paramagnetic susceptibility of the sample using the formula [46]

$$\chi = \frac{Ng^2\beta^2 J(J+1)}{3k_B T} \tag{10}$$

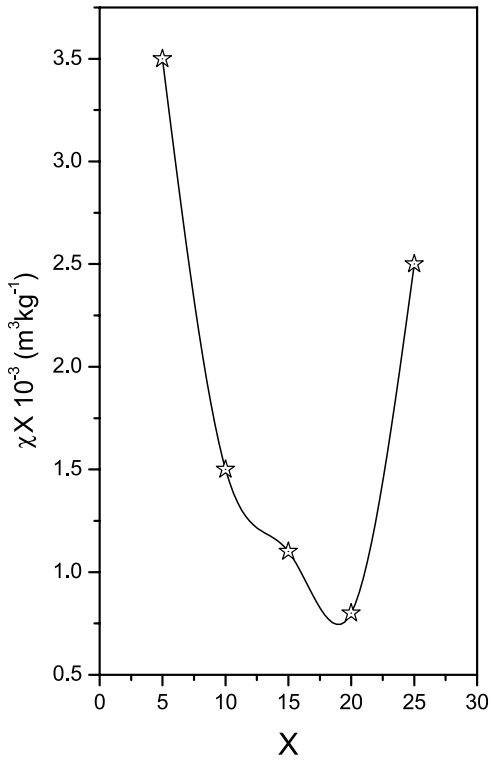

Figure 5. The variation of paramagnetic susceptibility (χ) with x in different mixed alkali borate glasses xNa$_2$O–$(30-x)$K$_2$O–69.5B$_2$O$_3$ + 0.5CuO ($5 \leqslant x \leqslant 25$), at room temperature.

Table 4. The number of Cu^{2+} ions (N_2), N_2/N_T and susceptibilities for 0.5 mol% CuO doped in the mixed alkali borate xNa$_2$O–$(30-x)$K$_2$O–69.5B$_2$O$_3$ glass as a function of x at room temperature.

Glass sample, x	Number of spins (N_2) (10^{21} kg^{-1})	N_2/N_T (10^{-2})	Susceptibility (χ) (10^{-3} m^3 kg^{-1})
5	12.4	0.342	3.5
10	5.5	0.149	1.5
15	4.1	0.108	1.1
20	2.8	0.068	0.8
25	9.1	0.231	2.5

where N is the number of spins per cubic metre and the other symbols have their usual meaning. N can be calculated from equation (9) and $g = (g_\parallel + 2g_\perp)/3$ is taken from EPR data. It is observed that the paramagnetic susceptibility shows MAE and this is shown in figure 5. From the figure it is observed that the susceptibility decreases with x and reaches a minimum around $x = 20$ and thereafter increases with x, showing the MAE in the glasses. The variation may be due to the structural changes with composition and also the modification of boron network with alkali content.

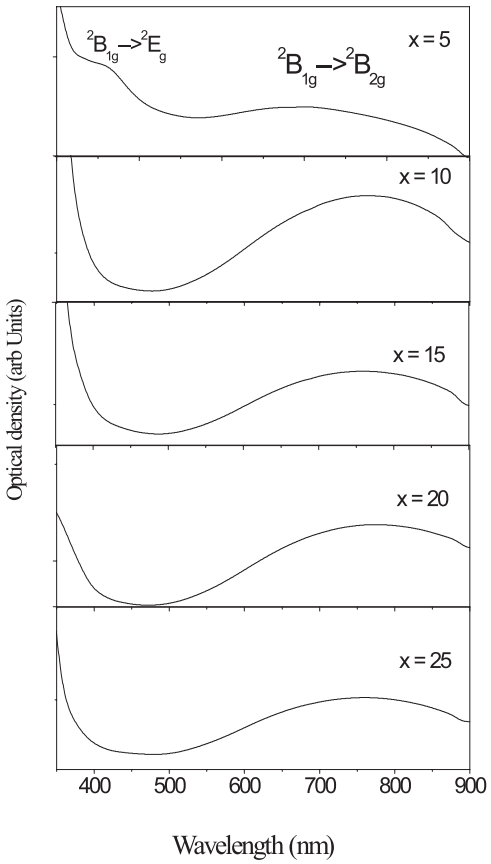

Figure 6. Optical absorption spectra of different mixed alkali borate glasses xNa$_2$O–(30 − x)K$_2$O–69.5B$_2$O$_3$ + 0.5CuO ($5 \leqslant x \leqslant 25$), at room temperature.

3.5. Optical absorption studies

The optical absorption spectra of Cu^{2+} ions in NaKB glasses at 300 K have been recorded in the wavelength region 300–900 nm and are shown in figure 6. The cuprous ion has the $3d^{10}$ configuration and consequently is not expected to have any ligand field band. The cupric ion, on the other hand, has the $3d^9$ configuration and the 3d level splits to ^2E_g and $^2T_{2g}$ in a ligand field of octahedral symmetry as shown in figure 7. However, as the ground state for divalent Cu in an octahedral ligand field is ^2E_g, tetragonal splitting due to Jahn–Teller distortion will occur and the ^2E_g level splits to $^2B_{1g}$ and $^2A_{1g}$ and the $^2T_{2g}$ level to $^2B_{2g}$ and ^2E_g as shown in figure 7. The difference in energy between $^2A_{1g}$ and $^2B_{2g}$ depends on the degree of distortion. However for sites of lower symmetry the theory predicts that more than one band will occur at energies higher than the octahedral transitions [9].

The optical absorption spectra (see figure 6) of all the samples are similar, showing one strong band corresponding to the $^2B_{1g} \rightarrow {}^2B_{2g}$ transition, except for $x = 5$ glass. For $x = 5$, two bands have been observed for the Cu^{2+} ion—a strong band corresponding to the transition ($^2B_{1g} \rightarrow {}^2B_{2g}$) centred at 14 240 cm^{-1} and a weak band corresponding to the transition ($^2B_{1g} \rightarrow {}^2E_g$) (22 115 cm^{-1}) on the higher energy side. For $x \geqslant 10$, the band $^2B_{1g} \rightarrow {}^2E_g$ vanishes, and the strong band shifts slightly to the lower energy side, centred

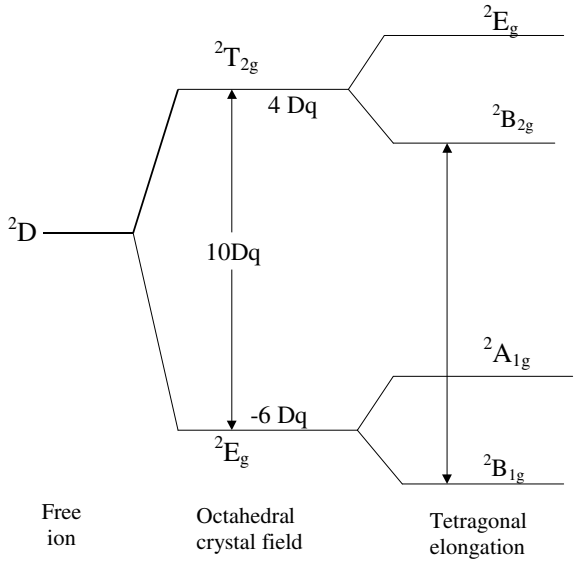

Figure 7. Schematic energy level diagram of Cu^{2+} in octahedral and tetragonal fields.

around 14 240–12 935 cm^{-1}. This shift can be attributed to the increase of ligand field around Cu^{2+} ion with increase of x.

The intensity of the band ($^2B_{1g} \rightarrow {}^2B_{2g}$) decreases with x, reaches a minimum at around $x = 15$ and thereafter increases. The peak energy of this band corresponds directly to the ligand field strength 10 Dq. The band is broad and asymmetric because of several overlapping symmetric bands due to the tetragonal distortion caused by the Jahn–Teller effect. The appearance of the additional band at 22 115 ($^2B_{1g} \rightarrow {}^2E_g$) for Cu^{2+} ions in $x = 5$ glass may be due to sites of lower symmetry around the Cu^{2+} ion. The observed optical absorption bands obtained in the present work are in good agreement with those reported by earlier workers [33–37].

3.6. Optical bandgap energy (E_{opt}) and Urbach energy

The study of optical absorption in the ultraviolet region is a useful technique to understand the electronic band structure in glasses. The optical absorption may be displaced in a number of ways as a function of photon energy $h\nu$. The most satisfactory results were obtained by plotting $(\alpha h\nu)^{1/2}$ as a function of $h\nu$ as suggested by Tauc *et al* [47] and discussed fully by Davis and Mott [48].

The study of the variation of optical bandgap with composition in oxide glasses gives information regarding the structure and the nature of bonds in the matrix. In order to examine the optical bandgap energy for these mixed alkali glasses, the optical absorption spectra were also recorded in the near ultraviolet region.

The absorption coefficient $\alpha(\nu)$ is given by [49]

$$\alpha(\nu) = (1/t)\log(I/I_0) \tag{11}$$

where t is the thickness of the sample and (I/I_0) corresponds to absorbance near the edge. $\alpha(\nu)$ can be related to optical bandgaps for direct and indirect transitions following Davis and Mott [48]

$$\alpha(\nu) = B(h\nu - E_{opt})^n/h\nu \tag{12}$$

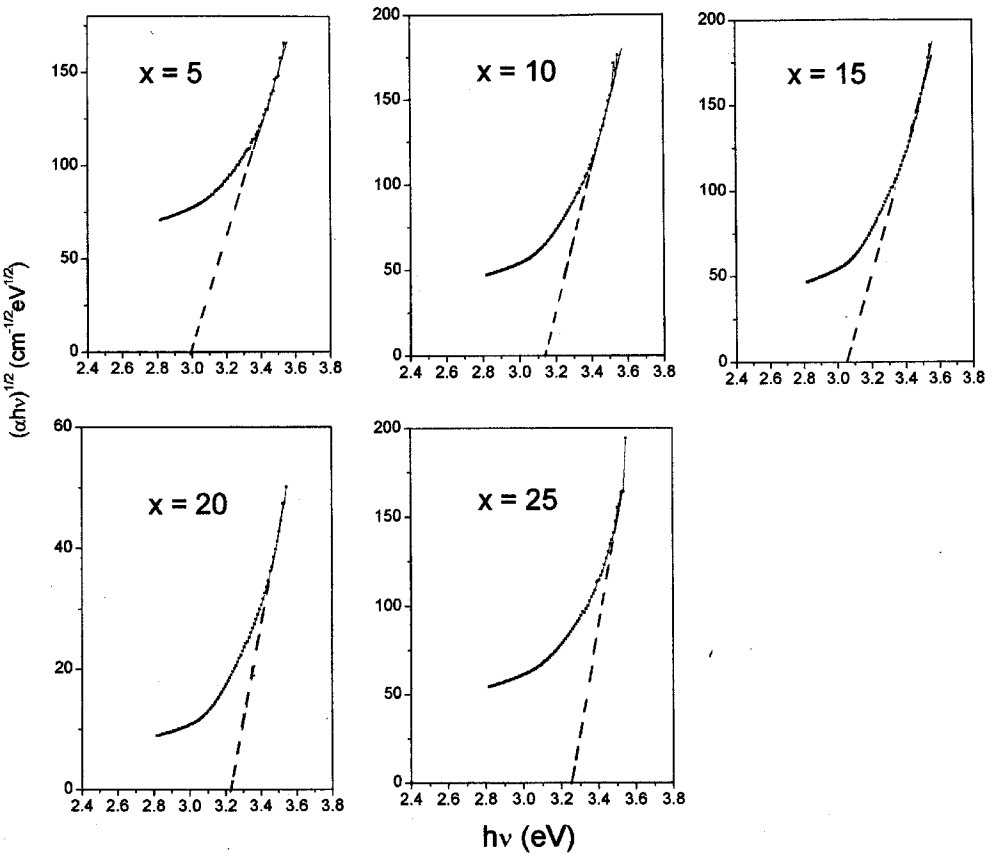

Figure 8. Plots corresponding to $(\alpha h\nu)^{1/2}$ versus $h\nu$ for different mixed alkali borate glasses $x\mathrm{Na_2O}$–$(30-x)\mathrm{K_2O}$–$69.5\mathrm{B_2O_3}$ + 0.5CuO ($5 \leqslant x \leqslant 25$), at room temperature (dotted curves are experimental points whereas the dashed one represents extrapolation to the linear region).

where B is a constant and E_{opt} is the energy of the optical bandgap and $h\nu$ is the photon energy of the incident radiation. For indirect transitions $n = 2$ and for direct transitions $n = 1/2$. From the plots of $(\alpha h\nu)^{1/2}$ and $(\alpha h\nu)^2$ as a function of photon energy $h\nu$, E_{opt} values can be obtained by the extrapolation of the linear region of the plots to the $h\nu$ axis for indirect and direct transitions and are shown in figures 8 and 9 respectively.

Therefore, the relation (12) can be readjusted to represent the linearity between $(\alpha h\nu)^{1/2}$ and $(h\nu - E_{opt})$ and one can determine the indirect optical bandgap values from the curves representing $(\alpha h\nu)^{1/2}$ as a function of photon energy $h\nu$, as shown in figure 8. Thus the data obtained from the edges were fitted to the equation

$$(\alpha h\nu)^{1/2} = \text{constant}\ (h\nu - E_{opt}) \tag{13}$$

for the linear regions of the curve in figure 8. The values of E_{opt} were obtained by the extrapolation of the linear region of the plots of $(\alpha h\nu)^{1/2}$ versus $h\nu$ to the $h\nu$ axis and are given in table 5 (with an estimated error of ± 0.01 eV). The data corresponding to the non-linear region of figure 8 were found to fit to a second-order equation of the type

$$(\alpha h\nu)^{1/2} = P + Q(h\nu) + R(h\nu)^2 \tag{14}$$

where P, Q and R are constants.

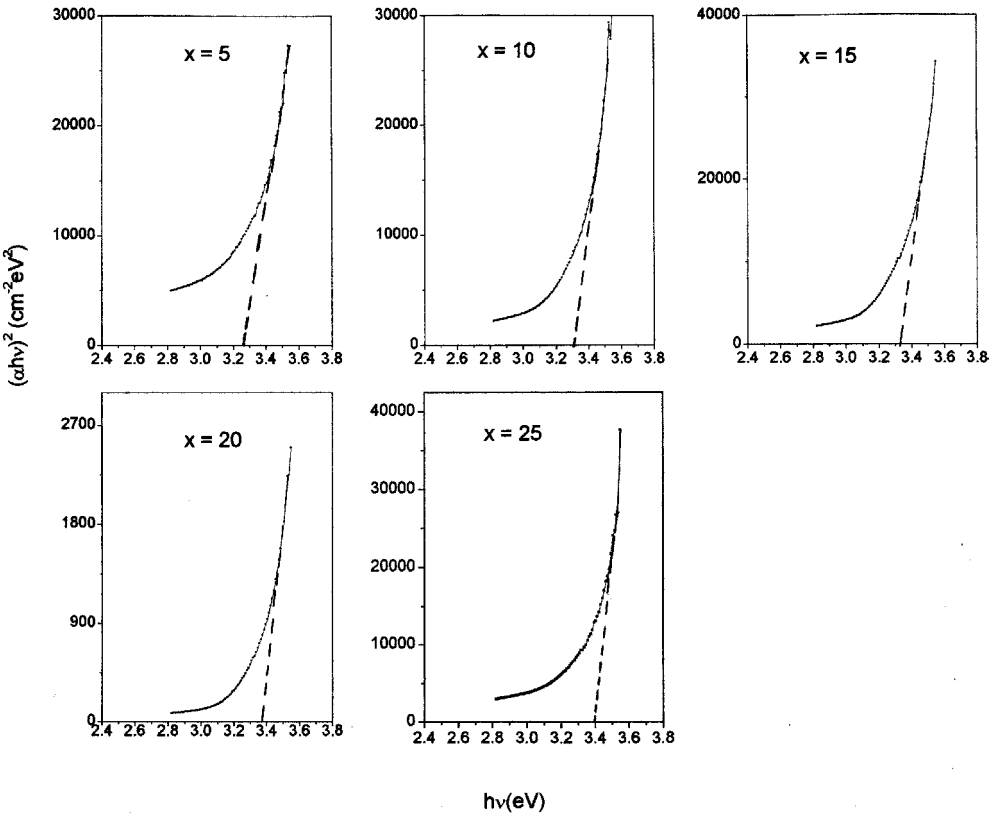

Figure 9. Plots corresponding to $(\alpha h\nu)^2$ versus $h\nu$ for different mixed alkali borate glasses $x\mathrm{Na_2O}$–$(30-x)\mathrm{K_2O}$–$69.5\mathrm{B_2O_3} + 0.5\mathrm{CuO}$ ($5 \leqslant x \leqslant 25$), at room temperature (dotted curves are experimental points whereas the dashed one represents extrapolation to the linear region).

It is to be noted that for lower values of the absorption coefficient $\alpha(\nu)$, the relation (12) gradually changes into an exponential dependence as given by the Urbach law [50]

$$\alpha(\nu) = \alpha_0 \exp(h\nu/\Delta E) \tag{15}$$

where α_0 is a constant and ΔE is the Urbach energy which indicates the width of the band tail of the localized states in the bandgap. The excitation levels at the absorption edges are determined by the random electric fields due to either the lack of long range order or the presence of defects [48, 51]

Plots were also drawn with $\ln(\alpha)$ against $h\nu$ (not shown in the figure) for the mixed alkali borate glasses in order to calculate the values of Urbach energy. The values of Urbach energy, ΔE, were calculated by determining the slopes of the linear regions of the curves and taking their reciprocals. The Urbach energies obtained for the glasses studied in the present work are also listed in table 5. The optical bandgap energies vary from 3.00 to 3.40 eV for both the direct and indirect transitions which is of the same order as expected for borate glasses.

3.7. Cu^{2+}–ligand bond nature

The metal–ligand bond nature can be described using the parameters α^2, β^2 and β_1^2 [52, 53]. The parameters α^2 and β_1^2 represent the contribution of 3d atomic orbitals of the cupric ion

Table 5. Molecular orbital coefficients and optical energy gaps.

Glass sample, x	α^2	β_1^2	$\Gamma\sigma$ (%)	$\Gamma\pi$ (%)	Optical bandgap energy (eV) Direct	Indirect	Urbach energy ΔE (eV)
5	0.734	0.943	58	11	3.27	3.00	0.11
10	0.730	0.898	59	20	3.30	3.14	0.19
15	0.746	0.879	55	24	3.33	3.06	0.18
20	0.751	0.886	54	23	3.38	3.23	0.23
25	0.737	0.903	57	19	3.40	3.25	0.17

to the B_{1g} and B_{2g} anti bonding orbitals respectively. The bonding coefficients α^2, β_1^2 and β^2 (=1.00) characterize, respectively, the in-plane σ bonding, in-plane π bonding and out-of-plane π bonding of the Cu^{2+} ligand bond in the glasses. The values of these parameters lie between 0.5 and 1.0, the limits of pure covalent and pure ionic bondings. A value of 0.5 represents a pure covalent bond while a value of zero or unity represents purely ionic bonding [53, 54]. The value of β^2 may be expected to lie sufficiently close to unity to be indistinguishable from unity in the bonding coefficient calculations [19]. The expression α^2 given in equation (16) is the bonding coefficient due to the covalency of the σ bonds with the equatorial ligands which measures the electron density delocalized on the ligand ions and β_1^2 accounts for covalency of π anti-bonding between ligands and the excited $^2B_{2g}$ state.

The bonding coefficient α^2 (i.e., the in-plane σ bonding) can be calculated from the EPR data using the expression given by Kuska *et al* [55].

$$\alpha^2 = \frac{7}{4}\left[\frac{A_\parallel}{P} - \frac{A}{P} - \frac{2}{3}g_\parallel - \frac{5}{21}g_\perp + \frac{6}{7}\right] \tag{16}$$

where $P = 0.036\,\mathrm{cm}^{-1}$ and $A = (1/3A_\parallel + 2/3A_\perp)$. The α^2 values calculated for mixed alkali borate glasses are presented in table 5.

The EPR and optical absorption spectral data can be correlated to evaluate the bonding coefficients as follows [53]:

$$g_\parallel = 2.0023\left[1 - \frac{4\lambda\alpha^2\beta_1^2}{E_1}\right] \tag{17}$$

$$g_\perp = 2.0023\left[1 - \frac{\lambda\alpha^2\beta^2}{E_2}\right]. \tag{18}$$

E_1 and E_2 are the energies corresponding to the transitions $^2B_{1g} \rightarrow {}^2B_{2g}$ and $^2B_{1g} \rightarrow {}^2E_g$ respectively, and λ is the spin–orbit coupling constant ($= -828\ \mathrm{cm}^{-1}$) [56].

From the equations (17) and (18) it can be seen that to determine Cu^{2+} bonding coefficients one needs, in addition to the EPR parameters, the energy positions of the absorption bands of Cu^{2+} which indicate the values of E_1 and E_2. Since we have observed only one absorption band corresponding to the $^2B_{1g} \rightarrow {}^2B_{2g}$ transition for most of the glasses, the position of the second band can be estimated by the approximation [54]

$$E(^2B_{1g} \rightarrow {}^2E_g) = \frac{2k^2\lambda}{2.0023 - g_\perp} \tag{19}$$

where k^2 is the orbital reduction factor ($k^2 = 0.77$) and λ is the spin–orbit coupling constant.

If $\alpha^2 = 1$, the bond would be completely ionic. If the overlapping integral were vanishingly small and $\alpha^2 = 0.5$, the bond could be completely covalent. However, because

the overlapping integral is sizeable, we cannot speak strictly of covalent versus ionic bonds but we can say that the smaller the value of α^2, the greater the covalent nature of the bond. The trend is in the expected direction. Cupric ion is a network modifier and B_2O_3 is a network former in respect of Cu^{2+}–O–B bonds. β_1^2 reflects the competition between the cupric ion and its neighbouring network former cations to attract the lone pairs of the intervening oxygen ions. The value of β_1^2 depends strongly on the network former. In the present work, the β_1^2 value decreases with x up to $x = 15$ and thereafter increases, showing the MAE. This change in β_1^2 is related to the change in B–O bonds. The values of the calculated parameter α^2 and β_1^2 obtained for various glasses indicate that the in-plane σ bonding is moderately covalent whereas the in-plane π bonding is significantly ionic in nature, and the ionic character slightly decreases up to $x = 15$ and thereafter slightly increases.

The normalized covalencies of the Cu(II)–O in-plane bonds of σ and π symmetry are expressed [20] in terms of bonding coefficients α^2 and β_1^2 as follows.

$$\Gamma\sigma = \frac{200(1-S)(1-\alpha^2)}{1-2S}\% \tag{20}$$

$$\Gamma\pi = 200(1-\beta_1^2)\% \tag{21}$$

where S is the overlapping integral ($S_{oxygen} = 0.076$). The normalized covalency values of the Cu(II)–O in-plane bonding of π symmetry ($\Gamma\pi$) thus calculated are given in table 5, and it is seen that the in-plane bonding of π symmetry increases from $x = 5$ to 15 and thereafter it decreases. The changes in β_1^2 are related to the changes in B–O bonds; there is a decrease in the strength of B–O bonds resulting in the increase of covalency of Cu(II)–O bonds. The Cu(II)–O bonds may be affected by the direct adjacent B–O bonds as well as by the slightly more distant ones [34].

4. Conclusions

(1) In summary, it is interesting to note that the MAE is revealed by several spectroscopic parameters and the changes in the properties we have investigated can be linked to structural modifications of the network resulting from the MAE.

(2) The Cu^{2+} ions are in tetragonally distorted octahedral sites (D_{4h}) elongated along the z-axis in all the glass samples with $d_{x^2-y^2}$ ($^2B_{1g}$) ground state.

(3) The spin-Hamiltonian parameter $g_\parallel$ goes through a minimum around $x = 10$–15 whereas $A_\parallel$ goes through a maximum around $x = 15$ showing the MAE. These changes are due to structural changes taking place with composition and also the modification of the boron network with alkali content.

(4) The number of spins participating in resonance (N_2) and the calculated paramagnetic susceptibility (χ) decrease with x, reach a minimum around $x = 20$ and thereafter they increase, showing the MAE in these glasses.

(5) The molecular orbital values α^2 and β_1^2 obtained for various glasses in the present work indicate that the in-plane σ bonding is moderately covalent and in-plane π bonding is significantly ionic in nature and the ionic character slightly decreases up to $x = 15$, and thereafter increases, showing the MAE in these glasses.

(6) It is interesting to note that for $x = 5$ glass, two bands were observed for the Cu^{2+} ion. A strong band corresponding to the transition $^2B_{1g} \rightarrow {}^2B_{2g}$ at (14 240 cm^{-1}) and a weak band corresponding to the transition ($^2B_{1g} \rightarrow {}^2E_g$) (22 115 cm^{-1}) on the higher energy side are observed. The additional band on the higher energy side is due to sites of lower symmetry around the Cu^{2+} ion. With $x \geqslant 10$, the $^2B_{1g} \rightarrow {}^2E_g$ band vanishes.

(7) From the observed UV absorption tails the optical bandgap energy was calculated for both direct and indirect transitions as a function of x: it varies from 3.00 to 3.40 eV.

Acknowledgments

RPSC thanks the Council of Scientific and Industrial Research (CSIR), New Delhi for the award of a Research Associateship and the Science and Engineering Research Council (SERC) DST, New Delhi for the award of a Fast Track research project under the Young Scientist scheme.

References

[1] Day D E 1976 *J. Non-Cryst. Solids* **21** 343
[2] Ingram M D 1987 *Phys. Chem. Glasses* **28** 215
[3] Ingram M D 1994 *Glasstech. Ber.* **67** 151
[4] Bunde A, Ingram M D and Maass P 1994 *J. Non-Cryst. Solids* **172–174** 1222
[5] Shelby J E 1997 *Introduction to Glass Science and Technology* (Cambridge: Royal Society of Chemistry)
[6] Turner W H and Turner J A 1972 *J. Am. Ceram. Soc.* **55** 201
[7] Sakka S, Kamiya K and Yoshikawa H 1978 *J. Non-Cryst. Solids* **27** 289
[8] Hosono H, Kawazoe H and Kanazawa T 1978 *Yogyo-Kyokai-Shi* **86** 567
[9] Ahmed A A, Abbas A F and Moustafa F A 1983 *Phys. Chem. Glasses* **24** 43
[10] Bendow B, Banerjee P K, Drexhage M G and Lucas J 1985 *J. Am. Ceram. Soc.* **65** C92
[11] Ohisti Y, Mitachi S and Tanabe T 1983 *Phys. Chem. Glasses* **24** 135
[12] Shelby J E and Ruller J 1987 *Phys. Chem. Glasses* **28** 262
[13] Klonkowski A 1985 *J. Non-Cryst. Solids* **72** 117
[14] Ahmed M M, Hogarth C A and Khan M N 1984 *J. Mater. Sci. Lett.* **19** 4040
[15] Guedes de Sousa E, Mendiratta S K and Machado da Silva J M 1986 *Port. Phys.* **17** 203
[16] Duffy J A and Ingram M D 1975 *J. Inorg. Nucl. Chem.* **37** 1203
[17] Pauling L 1960 *The Nature of Chemical Bond* 3rd edn (Ithaca, NY: Cornell University Press) p 93
[18] Imagawa H 1968 *Phys. Status Solidi* **30** 469
[19] Hosono H, Kawazoe H and Kanazawa T 1978 *J. Non-Cryst. Solids* **29** 173
[20] Hosono H, Kawazoe H and Kanazawa T 1979 *J. Non-Cryst. Solids* **34** 339
[21] Bandyopadhyay A K 1980 *J. Mater. Sci.* **15** 1605
[22] Sundar H G K and Rao K J 1982 *J. Non-Cryst. Solids* **50** 137
[23] Bogomolova L D, Fedorov A G and Kubrinskaya M E 1983 *J. Non-Cryst. Solids* **54** 153
[24] Klonkowski A 1985 *Phys. Chem. Glasses* **26** 11
[25] Klonkowski A 1985 *Phys. Chem. Glasses* **26** 31
[26] Yadav A and Seth V P 1986 *Phys. Chem. Glasses* **27** 182
[27] Yadav A and Seth V P 1987 *J. Mater. Sci.* **22** 239
[28] Yadav A, Seth V P and Chand P 1987 *J. Mater. Sci. Lett.* **6** 468
[29] Yadav A, Seth V P and Gupta S K 1988 *J. Non-Cryst. Solids* **101** 1
[30] Ramana M V, Siva Kumar K, Syed Rahman, Suresh Babu, Satyanarayan S G and Sastry G S 1989 *J. Mater. Sci. Lett.* **8** 1471
[31] Lakshmana Rao J, Sreedhar B, Ramachandra Reddy M and Lakshman S V J 1989 *J. Non-Cryst. Solids* **111** 228
[32] Narendra G L, Sreedhar B, Lakshmana Rao J and Lakshman S V J 1991 *J. Mater. Sci.* **24** 5342
[33] Rao A S, Lakshmana Rao J and Lakshman S V J 1992 *J. Phys. Chem. Solids* **53** 1221
[34] Biswas N C, Dayal R and Chand P 1996 *Phys. Chem. Glasses* **37** 31
[35] Shareefuddin Md, Vanaja K, Madhava Rao P, Jamal M and Narasimha Chary M 1998 *Phys. Chem. Glasses* **39** 184
[36] Sreekanth Chakradhar R P, Murali A and Lakshmana Rao J 1998 *J. Alloys Compounds* **265** 29
[37] Murali A and Lakshmana Rao J 1999 *J. Phys.: Condens. Matter* **11** 7921
[38] Kumar R R, Bhatnagar A K and Reddy B C V 2000 *Solid State Commun.* **114** 493
[39] Ardelean I, Peteanu M, Ciceo-Lucacel R and Bratu I 2000 *J. Mater. Sci. Mater. Electron.* **11** 11
[40] Ramadevudu G, Shareefuddin Md, Sunitha Bai N, Lakshmaipathi Rao M and Narasimha Chary M 2000 *J. Non-Cryst. Solids* **278** 205
[41] Ciorcas F, Mendiratta S K, Ardelean I and Valente M A 2001 *Eur. Phys. J.* B **20** 235

[42] Ravikumar R V S S N, Rajagopal Reddy V, Chandrasekhar A V, Reddy B J, Reddy Y P and Rao P S 2002 *J. Alloys Compounds* **337** 272
[43] Abragam A and Bleaney B 1970 *Electron Paramagnetic Resonance of Transition Ions* (Oxford: Clarendon) p 175
[44] Bleaney B, Bowers K D and Pryce M H L 1955 *Proc. R. Soc.* A **228** 147
[45] Weil J A, Bolton J R and Wertz J E 1994 *Electron Paramagnetic Resonance—Elementary Theory and Practical Applications* (New York: Wiley) p 498
[46] Aschcroft N W and Mermin N D 2001 *Solid State Physics* (Fort Worth, TX: Harcourt) p 656
[47] Tauc J, Grigorovice R and Vancu A 1966 *Phys. Status Solidi* **15** 627
[48] Davis E A and Mott N F 1970 *Phil. Mag.* **22** 903
[49] Sands R H 1955 *Phys. Rev.* **99** 1222
[50] Hassan M A and Hogarth C A 1988 *J. Mater. Sci.* **23** 2500
[51] Gan Fuxi D L 1992 *Optical and Spectroscopic Properties of Glass* (Berlin: Springer) p 62
[52] Maki A H and McGarvey B R 1958 *J. Chem. Phys.* **28** 31
[53] Kivelson D and Neiman R 1961 *J. Chem. Phys.* **35** 145
[54] Klonkowski A 1983 *Phys. Chem. Glasses* **24** 166
[55] Kuska H A, Rogers M T and Durllinger R E 1967 *J. Phys. Chem.* **71** 109
[56] Mabbs F M and Machin D J 1973 *Magnetism and Transition Metal Complexes* (London: Chapman and Hall) p 154